Proceedings of The National Conference
On Undergraduate Research (NCUR) 2014
University of Kentucky, Lexington
April 3-5, 2014

Computational Fluid Dynamics of the Pediatric Trachea

David Rutkowski
Department of Mechanical Engineering
Valparaiso University
1900 Chapel Drive
Valparaiso, IN 46383

Rapid Prototyping Center
Milwaukee School of Engineering
1025 N. Broadway
Milwaukee, WI 53202

Faculty Advisor: Dr. Subha Kumpaty

Abstract

This research analyzes the physical effects of a tracheal obstruction in the airway of a pediatric patient diagnosed with tracheomalacia. This condition causes a collapse of the trachea of young children, and is characterized by a lack of supporting cartilage in this region of the airway. The obstruction alters airflow and pressure throughout the remainder of the respiratory tract. Currently, medical professionals do not have a complete understanding of tracheomalacia. Additionally, the processes currently used to diagnose this condition are unpleasant for children, and in some cases aggravate the obstructed airway. In order to analyze the effects of tracheomalacia, computational fluid dynamics (CFD) was applied to study the airflow and pressure differences induced along the trachea. The process began by obtaining a computed tomography (CT) scan of the airway of a child with tracheomalacia. Using MIMICS (Materialise, Leuven, Belgium) software, the CT scan was converted into a three-dimensional (3D) computer model in standard transformation language (STL) format. Magics (Materialise, Leuven, Belgium) software was then used to refine the computer model. The STL file was then imported into CFD analysis software FLUENT (Ansys, Lebanon, USA). Airflow simulations were then run, and results were compared to properties of a normal airway and displayed through computer 3D modeling and visual representation. In order to provide a physical representation of the affected pediatric airway, physical 3D models were also created from the same STL files that were used for the CFD analysis, using the additive manufacturing process called selective laser sintering. The results of this research will provide further insight into the effect of airway obstructions, such as tracheomalacia, on the properties of airflow through pediatric airways.

Keywords: Computational Fluid Dynamics, Tracheomalacia, Airflow, Pediatric Airway, Selective Laser Sintering

1. Introduction

Airway obstructions in the respiratory tract of pediatric patients have long been a cause of concern among medical professionals. Such obstructions may cause a variety of symptoms and can be life-threatening. Many pediatric respiratory conditions can be easily diagnosed and treated, however, there are some conditions that are currently difficult to assess. One such condition prevalent in pediatric patients is known as tracheomalacia, a disorder characterized by the collapse of the trachea. Respiratory diseases such as this are usually diagnosed through the observation of medical images or through the use of airway probes. Although these methods are very useful in the detection of respiratory conditions, they do not provide all of the detail necessary to diagnose and properly treat rare disorders, such as tracheomalacia. Therefore, other methods must be pursued to provide adequate information to medical professionals. The objective of this research is to use one of these other methods, known as computational fluid dynamics (CFD), to analyze the effect an airway obstruction has on the flow properties of a pediatric airway affected by tracheomalacia. In order to give a physical representation of this condition, three-dimensional models were also produced using additive manufacturing technology. The results of this project will provide medical professionals with an alternative method in the analysis of airway disorders that may be used in training, demonstration, and treatment planning purposes.

1.1. Function Of The Human Airway

The human airway runs from the nasal cavity, down to alveoli in the lungs, and is the major component of the human respiratory system, as seen in Figure 1. This system provides the body with the oxygen necessary to live and rids it of respiratory waste [1]. Proper flow of these gases throughout the airway is highly dependent on the complex geometry of the airway components. Along the respiratory tract, the branches of the airway get narrower and more numerous. As a result, there is a change in total surface area, and in turn, a drop in pressure. This pressure drop is the driving force for airflow throughout the respiratory system [2]. Airflow properties are quantified by pressure and air velocity measurements along the respiratory tract. If part of the airway geometry is obstructed in any way, the airflow properties will change. This may result in breathing difficulties and reduced oxygen delivery to the body. Due to these potential risks, it is essential to know how airflow is affected by various respiratory conditions that alter the geometry of the airway. Although geometry changes can occur in any region of the respiratory tract, this research only analyzes the section of the airway from the top of the trachea to the first branching of the bronchi, as it is this section that is affected by tracheomalacia.

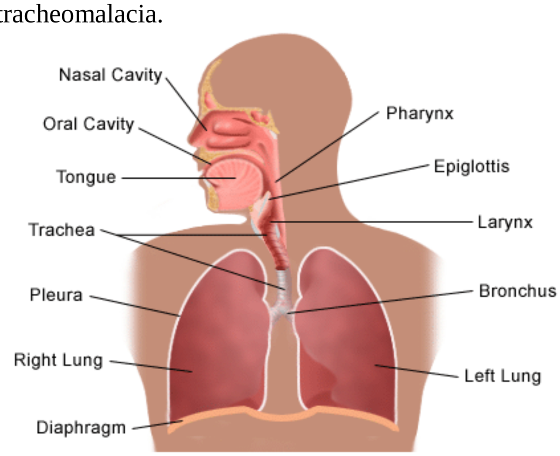

Figure 1. Anatomy of the Human Airway [3].

1.2. Tracheomalacia

Tracheomalacia is a rare condition that occurs predominantly in infants and young children. It is characterized by a collapse in the trachea, due to a deficiency of supporting cartilage. This collapse usually takes place while the child's breathing rate is high, such as when they are upset or crying. As a result of the collapse, the trachea often assumes a comma-shape. This reduces the diameter of the trachea, causing an increase in pressure drop across the region and a variance in airflow velocity. Such changes can lead to breathing difficulties and a lack of oxygen delivery. Consequently, the lack of oxygen may lead to brain damage, paralysis, and in extreme cases, death. Medical professionals are currently trying to better understand this condition. They are specifically looking for what airway properties cause the airway to collapse, and how it may relate to prevention and treatment. Up to now, the main form of investigation into this condition was through the use of bronchoscopy and medical images, such as magnetic resonance imaging (MRI), and computed tomography (CT) scans. Bronchoscopy is performed by feeding a bronchoscope down the airway of the patient. This allows the clinician to navigate the airway and see the inside of the respiratory tract. MR images and CT scans provide two-dimensional images of the whole airway anatomy at once and allow for the observation of anatomical irregularities. However, these techniques have limitations when it comes to diagnostics and treatment planning. Bronchoscopy can be difficult to perform on children who are uncooperative. Additionally, the physical contact of the bronchoscope with the airway can further aggravate the respiratory condition by adding extra stress to the tracheal wall. The disadvantage of CT and MR imaging is the two-dimensional format, which can make it difficult for doctors to pinpoint the location of the obstruction in three-dimensional space. Furthermore, these three diagnostic techniques do not provide information on the properties of air flow though the affected area [4-5].

1.3. Computational Fluid Dynamics

Fluid dynamics is the study of the flow phenomena of fluids. Analysis of fluid flow through, or around, various geometries allows scientists and engineers to see how certain conditions affect the performance of the object of study. The results of fluid dynamics studies are quantified by parameters such as flow velocity, air pressure, and surface stress. The relation between these parameters can be described by the Bernoulli Principle. This principle states that an equilibrium relationship exists between velocity and pressure – that is, as velocity increases, pressure will decrease, and vice versa. These properties can be calculated through either experimentation or mathematical equations. The main equations used for such mathematical calculations are known as the Reynolds Averaged Navier Stokes equations. Through these equations, a numerical quantification of flow intensity, known as the Reynolds Number, is calculated. Based on the magnitude of the Reynold's number, fluid flow is termed as either laminar or turbulent. Laminar fluid flow can be characterized as even and undisrupted. Conversely, turbulent flow can be described as chaotic and unpredictable [6].

For complex geometries, mathematical analyses can be very difficult. Furthermore, many real-life fluid dynamics situations require a turbulent air flow analysis method, rather than the more simplex laminar flow method. In these cases, it is necessary to apply computational methods to solve the problem. With the help of computer software, complex flow fields can be solved in a relatively short amount of time [6-7]. Many software packages allow the user to import a geometry file into the program. A computational mesh is then created, which specifies the level of precision at which the geometry will be analyzed. The program then requires user input of realistic physical parameters and boundary conditions, which are used in the flow calculations to give accurate results. The use of computational fluid dynamics has expanded to encompass the medical field over the last decade. In conjunction with proper medical image data and accurate boundary conditions, the software can be used to solve for flow fields in complex anatomical geometries. The results of the analyses are used to provide clinicians with flow properties that may be used in diagnoses, surgical planning, or treatment [8].

1.4. Additive Manufacturing

Additive manufacturing (AM) is the use of computer data to generate three-dimensional (3D) geometries. It is also known as rapid prototyping, or solid freeform fabrication. Additive manufacturing technology functions by taking thin cross-sections of 3D computer models, and translating this information into two-dimensional (2D) position data. This data is used to control the placement of a thin layer of material on the machine platform. Layers are continuously added until the object is complete [9]. There are several AM technologies available such as stereolithography (SLA), selective laser sintering (SLS), solider process, fused deposition modeling (FDM), laminated object manufacturing (LOM), 3-D printing, and multiphase jet solidification (MJS). The use of each method varies based on the desired object material, detail, production time, and cost. Additive manufacturing is used in research and in industry to reduce product development time and improve design. Applications of AM span across many industries, and have recently generated high interest in biomedical applications. This is due to the capability of the technology to quickly generate an accurate 3D representation of anatomical geometries that allows medical professionals to practice and plan for treatment and surgical procedures [10].

1.4.1. selective laser sintering

Selective laser sintering (SLS) uses a laser to heat particles of ceramic, plastic, or metal powder that are contained on a machine platform. The laser traces the 2D outline of an object layer in the powder bed. As the laser hits the particles, they heat up and fuse together. When the layer is completed, a new layer of powder is added and the process is repeated until the 3D model is complete. As a result of the compatibility of many materials with SLS, a variety of applications can be addressed. This method of AM is preferred for the creation of a durable model, with intricate detail [9]. Therefore, SLS is the method that best fits the objectives of the model created in this research. The set-up of this method is shown in Figure 2.

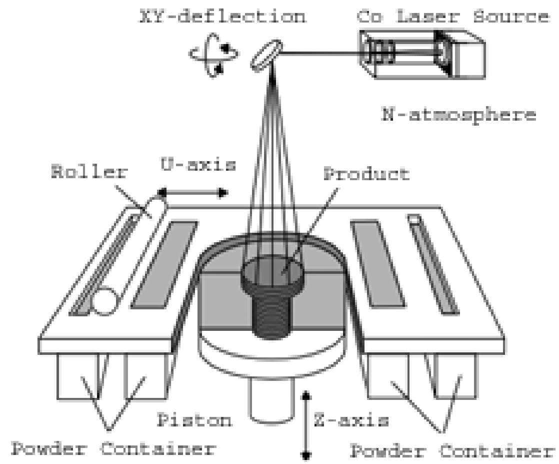

Figure 2. Overview of a selective laser sintering machine [9].

2. Methods

2.1. Data Acquisition

The data analyzed in this project was acquired from various sources. Data about boundary conditions relating to the airway geometries was adapted from previous research done by Luo et al. [11]. Numerical simulation parameters were also acquired, from Srivastav et al., including factors such as pressure, density, body forces, momentum, turbulent kinetic energy, turbulent dissipation rate, and turbulent viscosity [12]. The data for the normal pediatric airway, and the airway affected by tracheomalacia, was obtained through medical images provided by Dr. Ravindhra Elluru, pediatric otolaryngologist at Cincinnati Children's Hospital Medical Center. These medical image files were acquired through computed tomography (CT) scanning. Approval from the Institutional Review Board was granted for access of these de-identified files.

2.2. Data Processing

The CT medical images needed to be processed in order to be compatible with the CFD software and the selective laser sintering (SLS) machine. The CT scan data was acquired in digital imagine and communications in medicine (DICOM) format. The image slice data was saved in JPEG format, and then imported into MIMICS (Materialise, Leuven, Belgium) software. In this software, a tissue density threshold was selected to separate the trachea from the rest of the scan images. A 3D model was created from the selected CT area and saved in standard transformation language (STL) format. In order to refine the 3D model and make it compatible for production, the software program Magics (Materialise, Leuven, Belgium) was used. In this program, the model surface was fixed and smoothed to ensure adequate production on the SLS machine.

In order to make the model compatible with CFD software, further processing was required. In Magics software, the outer surface of the airway was removed, and the openings on each end of the airway were capped. The STL file was then imported into 3-matic (Materialise, Leuven, Belgium), where it was converted into Iges format. The file was then loaded into the ANSYS Dimension Modeler for a usable geometry to be created.

2.3. CFD Simulation

Once the geometry files were created, the models were ready to be processed using the CFD software, FLUENT (Ansys, Lebanon, USA). The files were transferred to the ANSYS Design Modeler, where meshes were created. The meshes were refined until the output of the results did not change. The final mesh size for the normal geometry was 304094 elements, and the final mesh size for the tracheomalacia obstructed geometry was 192265 elements. Each geometry was analyzed with both laminar and *k-ε* turbulent methods. The airway geometries were also both analyzed for inhalation and exhalation. The boundary conditions that were obtained through prior research documentation were then set [11-12]. An inlet velocity was set at the top opening of the trachea, and pressure outlets were set at the openings of the two main stem bronchi. The inlet velocity was set to 2.03 m/s, which simulates a high breathing rate. Air density was set to 1.19 kg/m^3, and viscosity to 1.82x10^{-5} kg/m-s. A no-slip wall boundary condition was set and a second order upwind numerical scheme was implemented. Under-relaxation factors were set at the following values: pressure = 0.3, momentum = 0.4, body forces = 0.5, density = 0.5, turbulent kinetic energy – 0.1, turbulent viscosity = 0.2 and turbulent dissipation rate = 0. The solutions were set to complete when the residuals converged to 10^{-4}.

3. Results

3.1. CFD

The first simulations run on the two pediatric trachea models were done to simulate inhalation, with a laminar flow method. When the results of the normal trachea were compared with the results of the tracheomalacia-affected trachea, significant observations were made with respect to the velocity and pressure behaviors.

The velocity vector simulation results gave insight on airflow patterns throughout both airways. As seen in Figures 3-4, there are major differences in the flow patterns between the normal and obstructed tracheas. The air velocity throughout the normal airway is relatively uniform throughout the length of the trachea. The air velocity is highest in the center of the trachea and shows no disruption patterns. However, the same is not true for the velocity vectors in the airway that is obstructed by tracheomalacia. In this airway, the velocity varies significantly throughout the trachea. Noting the different scales on each model, it can be seen that the air velocity at the inlet of each model is the same. However, in the airway with tracheomalacia, the air velocity significantly increases at the point of the obstruction. This velocity increase carries down into the bronchi, altering velocity throughout the rest of the respiratory system. Another consequence of the obstruction on the velocity vectors is the effect seen on air distribution through the two bronchi branches at the end of the trachea. As seen on the obstructed model, the airflow is almost completely directed into the right bronchi branch. This is presumed to be a partial result of the fact that the right bronchi branch is the larger of the two, thus providing less airflow resistance. In a real respiratory setting, this altered distribution of airflow would greatly affect respiratory function, as the left lung would not receive an adequate amount of air. In addition to air distribution, the velocity vectors reveal airflow disruptions due to air recirculation. On the obstructed model, small circular airflow patterns can be seen in the area of the trachea below the obstruction. These patterns would cause further breathing difficulties, as they show that some air would flow slightly back up the airway during inhalation.

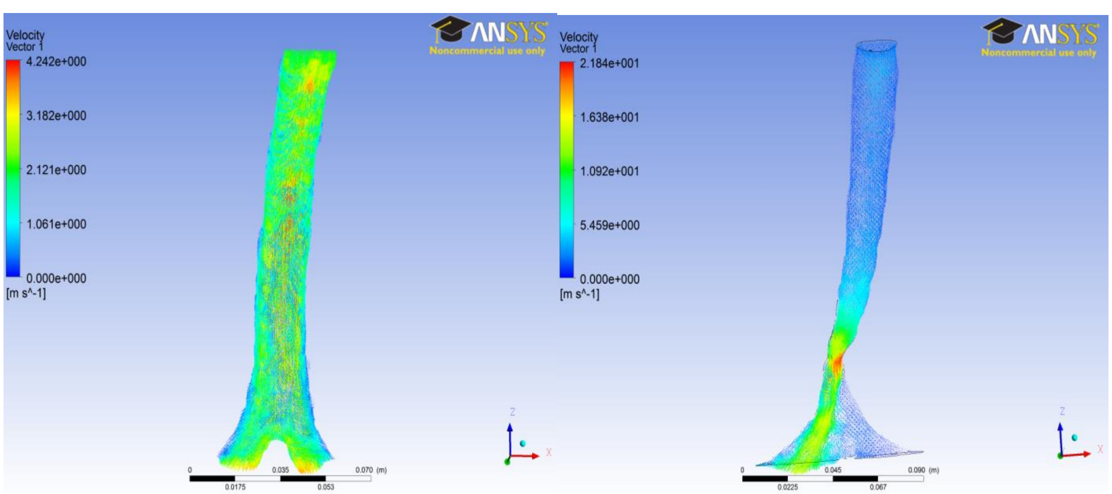

Figures 3-4. The velocity vectors in both a normal trachea (left) and an obstructed trachea with tracheomalacia (right). The models are in a front view, thus the left side of each model represents the right anatomical side.

The pressure contour simulation results also provided relevant insight on the function of an airway affected by tracheomalacia relative to a geometrically normal airway. As seen in Figures 5-6, the points of the lowest pressure correlate to the points of the highest velocity in Figures 3-4, displaying the Bernoulli principle. Also seen in Figures 5-6, the pressure distribution in the airway obstructed by tracheomalacia is considerably different than the distribution shown in the normal airway. The pressure throughout the normal airway is consistent. This is the desired pressure distribution for a trachea, as it offers a pressure drop from top to bottom, allowing air to flow properly. However, this preferred distribution is not seen in the pressure contours of the obstructed trachea. As seen in Figure 6, the pressure in the area above the obstruction is very high. The pressure then shows a significant drop at the point of the obstruction, and then increases again in the region below the obstruction. Due to this up-and-down pressure behavior, the pressure gradient is disrupted, and air does not flow properly. Additionally, the pressure contour results reveals insight on the pressure experienced by the walls of the trachea in an obstructed airway. Noting that the pressure contour scale is relative to atmospheric pressure, it can be seen that a negative pressure forms at the point of the obstruction. This inward pressure would cause further stress of the wall of the tracheomalacia affected region. The pressure increase at this point could cause further damage to the trachea, and lead to further collapse.

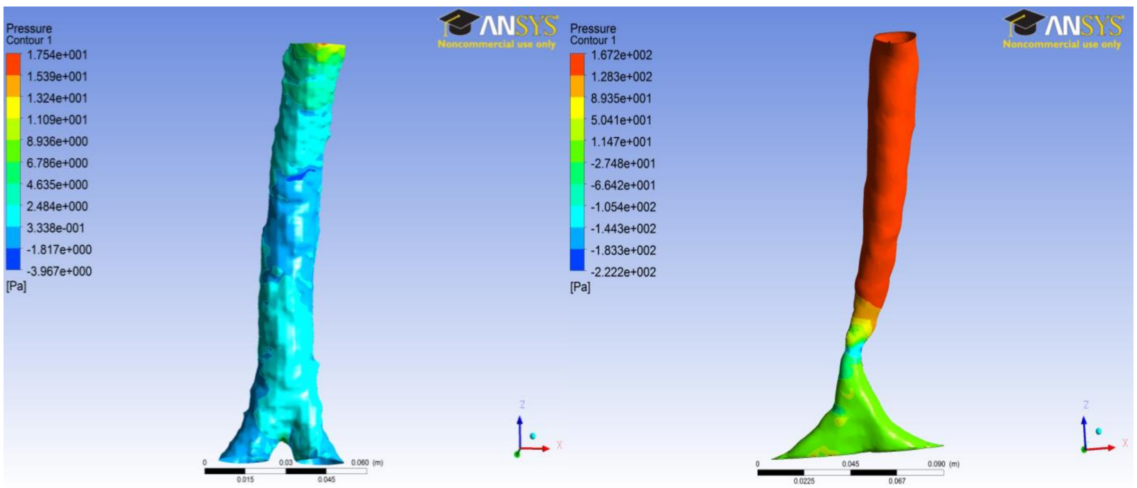

Figures 5-6. The pressure distribution in both a normal trachea (left) and a trachea obstructed by tracheomalacia (right). The models are in a front view, thus the left side of each model represents the right anatomical side.

In addition to the laminar inhalation simulation, exhalation and turbulent simulations were also run. These simulations showed similar patterns on the effect of an obstruction on air velocity and pressure. Thus, any differences that these simulations displayed are not discussed for the purposes of this research.

3.2. 3D Models

Two three-dimensional models of the pediatric airway were created in order to give a physical representation of the effects of tracheomalacia on the geometry of an airway. These models can be seen in Figures 7-8. One of the models represents a normal trachea of a child with no respiratory disorder. The other model represents a trachea of a child with tracheomalacia. The models were built using the Sinterstation 2500plus (3D systems), a machine that employs the selective laser sintering manufacturing technique. The material used for construction of these models was Duraform PA, a durable engineering plastic that allows for fine model detail. From the time that the computer data was transferred to the computer, the build time for these models was eight hours. Dimensions for the normal and tracheomalacia-affected airway are seven and five inches, respectively. The reason for the length difference is a result of the amount of image data available in the CT images provided. The scan of the child affected by tracheomalacia started higher in the throat area, allowing for additional length of the top end of the trachea.

Figures 7-8. Pictures of the three-dimensional models of a normal pediatric trachea (left) and a trachea affected with tracheomalacia (right), created with additive manufacturing technology.

4. Limitations

There were a number of limitations that affected the processes and outcomes of this research. The first limiting factor was data availability and detail. Medical images are often difficult to attain, especially if the image is for a specific condition or small part of the body such as the trachea. Additionally, many images do not provide adequate detail to analyze every aspect of the situation at hand. For example, in order to fully analyze the trachea, patient specific information on tracheal properties is needed. Furthermore, up-close detail of wall surfaces and grooves, such as tracheal cartilaginous rings, should be included to get more accurate results. Many medical images do not and cannot provide all of this information. Another limiting factor in this research was the availability of advanced technology. If all factors were taken into account when analyzing the airways and a more accurate mesh was used, then super-computing capabilities would be necessary. In many of the more complex airway projects done in past research, the computation time was very long, even with the use of a super-computer. The final limitation that should be presented is the initial lack of familiarity of the primary investigator with the programs used. Learning the program capabilities and properly importing data took a large amount of the time that was allotted for this project. As a result, the time spent on analyses was limited in comparison to preparation and set-up.

5. Conclusion

This research successfully modeled and analyzed realistic pediatric airway geometries using computational fluid dynamics. Through analysis, general conclusions can be made about the effects of airway obstruction due to tracheomalacia on the function of pediatric airways. Significant observations deal with the effect of an obstruction on the air velocity and pressure distribution of the airway. As stated, the pressure drop along the airway is the driving force for airflow. However, when the airway was obstructed, the pressure distribution was disrupted. In the obstructed model, the pressure values decreased and increased many times along the airway walls. As a result, the pressure did not decrease in a uniform manner from inlet to outlet. Additionally, the pressure variance had a direct impact on the walls of the airway. At the point of the obstruction, a negative pressure (relative to atmospheric pressure) formed. In a real airway situation, this would cause an inward force on the airway, and would pull it in, increasing the potential for collapse. As a consequence of the pressure variance, the airflow was sporadic throughout the airway. The re-circulation effect observed in the obstructed airway may cause a disruption in air distribution in real human trachea and bronchi. Despite the fact that all physical factors were not analyzed in these airway models, results were produced that may be helpful in clinical assessment of airway disorders, such as tracheomalacia.

6. Acknowledgements

The primary investigator would like to thank the National Science Foundation and the Milwaukee School of Engineering Rapid Prototyping Center for providing funding for the Research Experience for Undergraduates (REU) program. The investigator would also like to thank the advisor of this research project, Dr. Subha Kumpaty for the assistance and direction provided, and Dr. Ravindhra Elluru for providing the medical images and his valuable insight. The investigator is also appreciative of Ann Bloor, Betty Albrecht, and the entire REU and Rapid Prototyping staff for the support and assistance in this research.

This material is based upon work supported by the National Science Foundation under grant No. EEC-1062621. Any opinions, findings, and conclusions or recommendations expressed in this material are those of the author(s) and do not necessarily reflect the views of the National Science Foundation.

7. References

1. P. Monnier, "Applied Surgical Anatomy of the Larynx and Trachea." Pediatric Airway Surgery. 17.371 (2011)
2. Yang, X.L., Yang Liu, and H.Y. Luo, "Respiratory Flow in Obstructed Airways." Journal of Biomechanics. 39. (2006): 2743-2751.
3. Asthma. Yale Medical Group, Yale School of Medicine. Accessed: 1 Jul 2013. <http://www.yalemedicalgroup.org/stw/Page.asp?PageID=STW023908>.
4. V.M. McNamara, and D.C.G. Crabbe. "Tracheomalacia." Pediatric Respiratory Reviews. 5. (2004): 147-154.
5. James Austin, and Ali Tariq. "Tracheomalacia and Bronchomalacia in Children: pathophysiology, assessment, treatment and anaesthesia management. “Pediatric Anaesthesia." 13. (2003): 3-11.
6. Bruce R. Munson, Donald F. Young, et al. Fundamentals of Fluid Mechanics. 6th ed. Wiley, 2009.
7. Pijush K. Kundu, and Ira M. Cohen. Fluid Mechanics. 4th ed. (City: Elsevier, 2008). <http://www.knovel.com/web/portal/browse/display?_EXT_KNOVEL_DISPLAY_bookid=4380&VerticalID=0>.
8. Jan W. De Baker, Wim G. Vos, et al. "Clinical Applications of Image-based Airway Computational Fluid Dynamics: Assessment of Inhalation Medication and Endobronchial Devices." Medical Imaging. 7262. (2009).
9. "Solid Freeform Fabrication." Academics. Milwaukee School of Engineering. Accessed: 2 Jul 2013. <http://www.msoe.edu/academics/research_centers/reu/solid_freeform_fabrication.shtml>.
10. M. McGurk, A Amis, et al. "Rapid Prototyping Techniques for Anatomical Modelling in Medicine."Guys Hospital London. 79. (1997): 169-174.
11. X.Y. Luo, J.S. Hinton, et al. "LES Modeling of Flow in a Simple Airway Model." Medical Engineering and Physics. 26. (2004): 403-413.
12. Vivek Kumar Srivastav, Anuj Jain, et al., "CFD Modelling of Airflow in Human Respiratory System."International Conference on Mechanical Engineering. (2011)